



Published in final edited form as:

Bone. 2012 April ; 50(4): 954–964. doi:10.1016/j.bone.2011.12.013.

Bone Marrow-Derived Heparan Sulfate Potentiates The Osteogenic Activity Of Bone Morphogenetic Protein-2 (BMP-2)

Diah S. Bramono¹, Sadasivam Murali¹, Bina Rai¹, Ling Ling¹, Wei Theng Poh¹, Zophia Xuehui Lim¹, Gary S. Stein², Victor Nurcombe^{1,3}, Andre J. van Wijnen², and Simon M. Cool^{1,3}

¹Stem Cells and Tissue Repair Group, Institute of Medical Biology, A*STAR (Agency for Science Technology and Research), Biopolis, Singapore 138648

²Department of Cell Biology and Cancer Center, University of Massachusetts Medical School, Worcester, Massachusetts 01655

³Department of Orthopaedic Surgery, Yong Loo Lin School of Medicine, National University of Singapore, Singapore 119074

Abstract

Lowering the efficacious dose of bone morphogenetic protein-2 (BMP-2) for the repair of critical-sized bone defects is highly desirable, as supra-physiological amounts of BMP-2 have an increased risk of side effects and a greater economic burden for the healthcare system. To address this need, we explored the use of heparan sulfate (HS), a structural analog of heparin, to enhance BMP-2 activity. We demonstrate that HS isolated from a bone marrow stromal cell line (HS5) and heparin each enhances BMP-2-induced osteogenesis in C2C12 myoblasts, through increased ALP activity and osteocalcin mRNA expression. Commercially available HS variants from porcine kidney and bovine lung failed to generate similar effects. Heparin and HS5 influence BMP-2 activity by (i) prolonging BMP-2 half-life, (ii) reducing interactions between BMP-2 with its antagonist noggin, and (iii) modulating BMP2 distribution on the cell surface. Importantly, long-term supplementation of HS5 but not heparin greatly enhances BMP-2-induced bone formation *in vitro* and *in vivo*. These results show that bone marrow-derived HS effectively support bone formation, and suggests its applicability in bone repair by selectively facilitating the delivery and bioavailability of BMP-2.

Keywords

heparan sulfate; heparin; BMP-2; glycosaminoglycan; osteogenesis

Introduction

Bone morphogenetic protein-2 (BMP-2) has been shown to be efficacious for the treatment of critical-sized bone defects with results comparable to autologous bone graft⁽¹⁻³⁾. As BMP-2 treatment replaces the need for autologous bone graft, its use is associated with shortened hospital stays for patients⁽⁴⁾. However, the high dose of BMP-2 required for a successful therapy carries with it an increased risk of side effects and a greater economic

Address correspondence to: Simon M. Cool, 8A Biomedical Grove, #06-06 Immunos, Singapore 138648, Singapore. Phone: +65 6407 0176; Fax: +65 6478 9477; simon.cool@imb.a-star.edu.sg.

Disclosures

All authors state that they have no conflicts of interest.

burden for the healthcare system⁽⁴⁾. To reduce the efficacious dosage, efforts have focused on improving BMP-2 half-life and/or sustaining and localizing its release⁽⁵⁻⁹⁾. Heparin, a hyper-sulfated glycosaminoglycan (GAG) sugar harvested from mast cell-rich tissues, has been investigated extensively and shown great promise in this regard. Heparin can bind to and modulate various extracellular molecules including growth factors, adhesion molecules, and receptors⁽¹⁰⁾. Heparin binds to and stabilizes BMP-2^(9,11) and reduces inhibition by the antagonist noggin^(11,12), thereby enhancing its osteogenic activity. It has also been suggested that heparin prevents BMP-2 from binding to endogenous cell-surface heparan sulfate proteoglycans (HSPGs), thus enhancing its bioavailability⁽⁹⁾. The use of heparin in bone repair has been extended to various types of scaffolds as a means to increase the incorporation of BMP-2 and sustain its delivery *in vivo*, thereby improving BMP-2 efficacy^(5,7,13-15).

Despite promising results, the use of heparin to augment BMP-2 therapy may pose unwanted effects due to heparin's affinity for a wide range of proteins. For instance, heparin's ability to interact and activate antithrombin III promotes its wide use in anti-coagulant therapy⁽¹⁶⁾. As the fracture hematoma acts as a reservoir for cytokines and growth factors important for bone repair⁽¹⁷⁾, the use of anti-coagulant compounds like heparin may be counter-productive. Furthermore, heparin treatment is known to reduce bone density and has been linked to the development of osteoporosis^(18,19) through its pro-osteoclastic actions *in vitro*^(20,21) and *in vivo*⁽¹⁹⁾. Indeed, heparin is known to inhibit the interaction between receptor activator of NF- κ B ligand (RANKL), a cytokine responsible for the formation and activation of osteoclasts, and its decoy receptor osteoprotegerin⁽²²⁾.

The current work identifies a novel heparan sulfate (HS) that stabilizes and enhances BMP-2 activity. Like heparin, HS is a GAG sugar with repeating disaccharide units of N-glucosamine and uronic acid. Importantly however, HS is less sulfated (40-60%) compared to heparin (>80%), and has a greater variability in its sulfation pattern⁽¹⁰⁾ that is critical for binding specific signaling molecules⁽²³⁾. This specificity is of major biomedical significance, because HS retains the advantageous bioactivity of heparin without the adverse effects associated with its pleiotropic protein affinity.

In this study we isolated HS from a stromal cell line derived from the human bone marrow microenvironment, an active site for the regulation of hematopoiesis and bone remodeling. The HS was characterized based on: (i) disaccharide composition and interactions with BMP-2, (ii) BMP-2 potentiating effects compared to commercially available heparin and HSs and (iii) the mechanisms responsible for enhancing BMP-2 activity. We hypothesized that bone marrow-derived HS provides a more physiologically relevant substrate compared to heparin in potentiating BMP-2 activity with minimal side effects.

Materials and Methods

Materials

All cell culture reagents were purchased from Gibco unless stated otherwise. All purified recombinant proteins were purchased from R&D Systems, Inc. Commercial porcine intestinal mucosa-derived heparin and HS (pHS), and bovine kidney-derived HS (bHS) were purchased from Sigma-Aldrich. All cell lines were purchased from American Type Culture Collection (ATCC).

Cell culture

The immortalized human bone marrow stromal cell line (HS-5, ATCC CRL-11882), herein referred to as BMS5 was maintained in DMEM (Sigma-Aldrich), 10% FCS (Lonza Group Ltd.), 100 U/mL penicillin/streptomycin (P/S), 4 mM L-glutamine and 1.5 g/L NaHCO₃.

Myoblast C2C12 cell was maintained in DMEM, 10% FCS and 100 U/mL P/S. Chinese Hamster Ovary (CHO) K1 and pgsD 677 cells were maintained in Ham's F-12 medium (Invitrogen), 10% FCS and 100 U/mL P/S. All cells were maintained at 37 °C/5% CO₂.

Unless stated otherwise, C2C12 cells were seeded at 2×10^4 cells/cm² in 24-well plates in maintenance media. Post-seeding (24 h), the culture media was replaced with treatment media (maintenance media with FCS reduced to 5%) in the presence/absence of 100 ng/mL BMP-2 and varying concentrations of noggin and GAGs. The cells were cultured in treatment media for 3 days and immediately assayed.

Collection of cell conditioned media

Cells were plated at 3×10^4 cells/cm² in maintenance media. After 24 h, the media was changed to treatment media and the conditioned media collected 24 h later, centrifuged at 3000 rpm for 5 min to remove any cell debris, then passed through a 0.45 µm filter, and stored at -20 °C. The conditioned media was then thawed and mixed (1:1 ratio) with fresh treatment media prior to being introduced to the culture in the presence/absence of BMP-2.

Heparan sulfate isolation and purification

Heparan sulfate was isolated and purified from the conditioned media of BMS5 cells as previously described⁽²⁴⁾. Briefly, BMS5 was seeded at 3×10^4 cells/cm² in 15-cm dish in maintenance media. The media was replaced the following day with serum free media and collected every other day up to day-11 and pooled. At each collection point, the media was centrifuged and filtered to remove cell debris. The extraction and purification of BMS5-derived HS (herein referred to as HS5) and its molecular weight and disaccharide unit analysis were as previously described⁽²⁵⁾.

GAG biotinylation

GAG was biotinylated according to methods described by Osmond *et al.* with some modifications⁽²⁶⁾. Briefly, 1 mg of sugar in 100 µL of 0.1 M 4-morpholinoethanesulfonic acid (MES), pH 5.5, was mixed with 30 µL of 2 mg/mL biotin-LC-hydrazide (Pierce Chemical Co.) dissolved in MES, and 0.75 mg 1-ethyl-3-(3-dimethylaminopropyl)carbodiimide hydrochloride (EDC), and incubated at room temperature for 2 h. Subsequently, another 0.75 mg of EDC was added and incubated for additional 2 h. The biotinylated GAGs were then purified using a fast desalting column (GE Healthcare).

Dot blot assay

To determine GAG binding to BMP-2, 0.5 µg of BMP-2 in 200 µL PBS was added under vacuum onto a nitrocellulose membrane. The blot was blocked with 5% BSA in PBS prior to incubating each BMP-2 spot with 1 µg of biotinylated GAG in 200 µL PBS. The bound biotinylated GAG was detected using HRP-conjugated streptavidin (BD Pharmingen).

GAG binding assay

The interaction between GAG and BMP-2 was determined using GAG binding plates (Iduron) according to the manufacturer's specification. GAG (10 µg/mL) was incubated in the plate prior to adding BMP-2. Bound BMP-2 was detected using biotinylated anti-BMP-2 antibody (R&D Systems) and AP-conjugated ExtrAvidin (Sigma-Aldrich).

Alkaline phosphatase activity

Cell layer was washed in PBS before lysis in RIPA buffer in the presence of protease inhibitor cocktail (Calbiochem). The protein content was determined using BCA protein

assay kit (Pierce Chemical Co.). ALP activity was measured by mixing 7 to 10 μg of protein with *p*-nitrophenylphosphate (Zymed). Enzyme activity was measured as a change in absorbance at 405 nm due to the production of *p*-nitrophenol per μg protein and normalized to treatment containing BMP-2 alone.

Real-time PCR

Total RNA was isolated and reverse transcribed as previously described⁽²⁷⁾. Expression level of target genes was determined using real-time PCR by amplification in ABI Prism 7500 FAST® sequence detection system (Applied Biosystems Inc.) using primers/probes for RUNX2 and osteocalcin as described previously⁽²⁷⁾ and Taqman Gene Expression Assays (Applied Biosystems Inc.) for β -actin and GAPDH. $2^{-(\Delta\text{Ct})}$ values from biological triplicates were measured in triplicates and normalized to β -actin and GAPDH levels to represent relative expression unit (REU).

Mineralization assay

Myoblast C2C12 cells were seeded at 5×10^3 cells/cm² in 24-well plates in maintenance media. After 24 h, the media was replaced with osteogenic media (DMEM, 5% FCS, 50 $\mu\text{g}/\text{ml}$ ascorbic acid and 10 mM β -glycerophosphate) in the presence/absence of 100 ng/mL BMP-2 and 3 $\mu\text{g}/\text{mL}$ GAG. The media was changed every 2 days. After 14 days, the cell layer was washed with PBS, fixed with 4% paraformaldehyde, and stained for 10 min in 0.1% alizarin red solution.

BMP-2 stability assay

BMP-2 at 100 ng/mL was incubated alone or in the presence of 3 $\mu\text{g}/\text{mL}$ of GAG in treatment media at 37 °C/5% CO₂. The media was collected at an indicated time and stored at -80 °C prior to BMP-2 quantification. The amount of BMP-2 present in the media was assayed using a BMP-2 Quantikine ELISA kit (R&D Systems) according to the manufacturer's specification.

BMP-2 activity

C2C12 cells were seeded on 24-well plates as described earlier. BMP-2 in treatment media was prepared as described in the BMP-2 stability assay for an indicated amount of time. Prior to adding the media containing BMP-2, the cell layer was pre-incubated with fresh treatment media for 24 h. The cells were then subjected to BMP-2-containing media for 15 min and the cell layer was lysed in Laemmli buffer, resolved in a 4-12% SDS-PAGE gel, and immunoblotted with antibodies against Smad 1/5/8 (Santa Cruz Biotechnology) and phosphorylated Smad 1/5/8 (Cell Signaling Technology).

Immunoprecipitation and western blot

BMP-2 (200 ng/mL) was incubated with Fc-conjugated noggin (600 ng/mL) in the presence/absence of 6 $\mu\text{g}/\text{mL}$ GAG. BMP-2 (100 ng/mL) was incubated with Fc-conjugated BMPR-IA (640 ng/mL) in the presence of 3 $\mu\text{g}/\text{mL}$ GAG. The complex formed was immunoprecipitated with protein A/G sepharose beads (Santa Cruz Biotechnology) for 1 h at 4 °C. The precipitated sample was then analyzed in a 4-12% SDS-PAGE and immunoblotted using anti-noggin (Millipore), anti-human IgG for BMPR-IA (eBioscience), and anti-BMP-2 (R&D Systems, Inc.) antibodies. Densitometry analysis using Quantity One software (Bio-Rad) was performed on 3 separate experiments to arrive at a mean value. The relative amount of bound BMP-2 was calculated by first, normalizing each BMP-2 densitometry value to its respective noggin or BMPR-IA densitometry value. Subsequently, the calculated value obtained is normalized to the treatment group containing no GAG.

FACS

Cultured cells were detached using 5 mM EDTA in RPMI 1640 containing 10% FCS and 32 mM HEPES. The detection of heparan sulfate proteoglycan on the surface of wild-type CHO K1 and heparan sulfate-deficient pgsD 677 cells was performed as previously described⁽²⁸⁾. To detect BMP-2 bound to the cell surface, 20 ng BMP-2 was pre-incubated with 1 µg anti-BMP-2 antibody before incubation with GAG. The cells were incubated with the BMP-2/antibody/GAG mixture in RPMI 1640/10% FCS for 1 h on ice. Secondary antibody was introduced as previously described⁽²⁸⁾.

Anti-coagulation assay

GAGs were assessed for their effect on antithrombin III activity. The assay was performed using the COATEST Heparin kit (Chromogenix) according to the manufacturer's specification. Values were represented as the relative inhibition of Factor Xa activity when compared to treatment group containing no GAG.

In vivo implantation

HELISTAT® collagen sponges (Integra Life Sciences Corp, USA) measuring 3.5 × 7 × 5mm were pre-soaked in 5 µg BMP-2 in the presence/absence of 25 µg of GAG (i.e. heparin, HS5 or bHS) and inserted into polycaprolactone (PCL) tubes (Osteopore International Pte Ltd, Singapore) measuring 4.5mm inner diameter, 3mm height and 1mm wall thickness. Collagen sponges pre-soaked in PBS served as a control. Porcine-derived HS was eliminated from the *in vivo* experimental setup since it consistently generated similar effects as bHS. Bilateral hind limb muscle pockets (2 in each limb) were created in 7 female Sprague Dawley rats (weighing 120-150g)⁽²⁹⁾ and randomly assigned to an experimental treatment. Pockets were created in the muscle by blunt dissection parallel to the muscle fiber long axis after creating 1cm transverse incisions over each muscle. All surgical procedures were carried out under general anesthesia and aseptic conditions. Anesthesia prior to surgery and its maintenance throughout surgery was achieved with isoflurane administration via an induction chamber and facemask. Prophylactic antibiotics (Baytril, 10mg/kg) and analgesics (Buprenorphine, 0.01-0.05mg/kg) were administered subcutaneously for 3 days post-surgery. Surgeries were performed in strict accordance with guidelines approved by A*STAR's Institutional Animal Care and Use Committee.

Bone formation analysis

The rats were sacrificed and specimens harvested 8 weeks after implantation. Three samples per treatment were assessed using 2D x-rays, µ-CT and histology for bone mineralization. An Imaging Radiographic System (MUX-100, Shimadzu) was used to capture 2D x-ray images of the muscle pockets immediately after the surgery and at week 8. Digital micrographs were then taken of the x-rays. Micro-CT images were captured with a µ-CT scanner (Skyscan 1076; Skyscan, Belgium) and analyzed using Mimics 13.1 software (Materialise, Belgium) as previously described⁽³⁰⁾. The data was recorded as total bone volume (mm³).

For histological analysis, the extracted specimens were fixed in 10% neutral buffered formalin for 1 week under vacuum, and decalcified in 30% formic acid for 2 weeks at room temperature. The specimens were then processed using a vacuum infiltration processor (Sakura Finetek, Japan), followed by dehydration, clearing, and embedding in Paraplast® paraffin wax (Thermo Scientific) as previously described⁽³⁰⁾. Sections were made using a rotary microtome (Leica Microsystems, Germany), placed onto microscope slides, stained with Hematoxylin/Eosin or Modified Tetrachrome⁽³¹⁾ and viewed with an Olympus upright fluorescence microscope (BX51).

Statistical analysis

Experiments were performed in duplicate or triplicate samples and repeated 2 to 3 times. Mean differences between samples were analyzed using SPSS statistics software by performing an exploratory data analysis and homogeneity of variance test, followed by ANOVA and Tukey's or Games-Howell posthoc testing. Statistical significance was defined at $p < 0.05$.

Results

Conditioned media from human bone marrow stromal cell line (BMS5) enhances BMP-2 activity

Conditioned media derived from C2C12 and BMS5 cells was added to C2C12 cells in the presence/absence of BMP-2. In the absence of BMP-2, none of the conditioned media induced ALP activity (**Fig. 1A**). However, in the presence of BMP-2, only BMS5 conditioned media significantly enhanced ALP activity above BMP-2-induced levels.

To determine whether HSPGs might constitute part of the active component of the BMS5 conditioned media, mRNA transcript expression of the three major families of HSPGs was examined as a prelude to isolating HS from the conditioned media (**Fig. 1B**). All the HSPG isoforms for glypican and syndecan, with the exception of glypican-3 and syndecan-3, were expressed in BMS5. Notably, the soluble HSPG isoform perlecan was abundantly expressed.

Following HSPG gene profiling, HS was isolated from BMS5 conditioned media (termed HS5) and subjected to molecular weight distribution and disaccharide analysis. The molecular weight of HS5 was distributed at 7.5, 29 and 75 kDa and the major disaccharide units were uronic acids linked to non-sulfated glucosamines or 6-O sulfated glucosamines (**Table. 1**). This is in contrast to heparin, which mainly consists of tri-sulfated disaccharide units⁽³²⁾. The identity of a portion of the disaccharide units retrieved could not be determined due to the current lack of standards for all possible combinations of variably sulfated disaccharide units and was omitted from the percent composition calculation.

GAG binds to BMP-2 at varying capacity

The ability of HS5 to bind BMP-2 was compared with commercially available GAGs using a GAG binding plate assay (**Fig. 1C**). Irrespective of the GAG variant used to coat the plate surface, BMP-2 bound to the immobilized GAG in a dose dependent manner. When GAG was omitted, minimal BMP-2 binding was detected. Furthermore, heparin, pHS and bHS bound more BMP-2 than did HS5, irrespective of dose.

To exclude the possibility that less HS5 bound to the GAG plate and thereby reducing the amount of bound BMP-2, we performed a nitrocellulose dot blot assay using immobilized BMP-2 as the capture substrate. The result confirms that more heparin binds to BMP-2 compared to HS5 (**Fig. 1D**)

HS5 enhances BMP-2-induced osteogenesis

Having established that HS5 binds to BMP-2, we next sought to determine the short-term effect of this interaction on BMP-2 activity. Using ALP activity assays, all GAGs tested dose-dependently increased BMP-2-induced ALP activity to levels significantly higher than BMP-2 alone in C2C12 myoblast cells after 3 days culture. Furthermore, the combination of either heparin or HS5 with BMP-2 resulted in more ALP activity compared to pHS and bHS at doses above 0.3 $\mu\text{g/ml}$ (**Fig. 2A**). GAG alone had no effect on ALP activity.

To further assess the effect of GAG/BMP-2 combinations on osteogenic differentiation, we examined the mRNA expression of early (RUNX2) and late (osteocalcin) osteogenic markers after 3 days. Either heparin or HS5 elevates osteocalcin mRNA expression by ~2-fold above BMP-2 treatment alone (**Fig. 2B**). This same dose of BMP-2 maximally induces RUNX2 transcript expression, because neither heparin nor HS5 had any additional effect, while pHS and bHS actually reduce RUNX2 mRNA expression.

Because heparin and HS5 enhance BMP-2 activity after 3 days, we determined their long-term effects on matrix mineralization (reflecting terminal differentiation) by Alizarin Red staining after 14 days of culture (**Fig. 2C**). Strikingly, long-term HS5 supplementation greatly enhances BMP2 stimulated matrix mineralization, but heparin, pHS or bHS do not. Matrix mineralization was observed as early as 6 days of culture when cells were stimulated with a combination of BMP-2 and HS5, a result not observed for the other treatments (data not shown). Interestingly, although pHS and bHS decrease RUNX2 and/or osteocalcin mRNA levels, neither compound inhibits BMP2 stimulated matrix mineralization.

HS5 prolongs BMP-2 stability and activity

We next tested whether HS5 stabilizes BMP-2. The amount of BMP-2 detected in treatment media decreased to approximately 50% and 3.5% of the starting amount within 2 and 72 h incubation respectively (**Fig. 3A**). In the presence of heparin, however, 85% of BMP-2 could be detected after 2 h and 17% after 72 h. In comparison, HS5 had no effect on the amount of BMP-2 detected for the first 8 h. However, from 8 h onwards, the loss of BMP-2 slowed to reach 15% of the original amount after 72 h, a level comparable to heparin. By taking into account the initial and final amount of BMP-2 present in solution after 48 h, the apparent half-life of BMP-2 ($t_{1/2} \approx 10$ h) improves by approximately 2-fold in the presence of heparin ($t_{1/2} \approx 22$ h) or HS5 ($t_{1/2} \approx 18$ h). Neither pHS nor bHS affected BMP-2 stability.

To further examine whether remaining BMP-2 detected in ELISA is still active, we tested BMP-2-induced Smad 1/5/8 phosphorylation (p-Smad 1/5/8) in C2C12 cells using BMP-2 or BMP-2/GAG combinations that had been incubated for 24 or 72 h (**Fig. 3B**). BMP-2-induced p-Smad 1/5/8 activity was comparable among all 24 h samples, while minimal p-Smad 1/5/8 activity was observed in the absence of BMP-2. Exposure to 72 h samples showed elevated p-Smad 1/5/8 activation in BMP-2 samples incubated with heparin or HS5 only. The samples contain 18 and 8 ng/mL BMP-2, respectively (**Fig. 3A**). In samples with BMP-2 alone (4 ng/mL) p-Smad 1/5/8 levels are just barely above basal levels suggesting that a threshold amount of BMP-2 (approximately 8 ng/mL) is required for robust Smad 1/5/8 signaling. Taken together, heparin and HS5 significantly prolongs BMP-2 osteogenic signaling activity through its stabilization.

GAGs modulate BMP-2 bioavailability

Since BMP-2 is known to bind to endogenous HSPGs on cell surfaces⁽³³⁾, we next examined whether exogenous GAGs could compete for this interaction, thus rendering BMP-2 more bioavailable. Using wild type (CHO K1) and HSPG-deficient mutant (pgsD 677) CHO cells, we confirmed that BMP-2 bound to endogenous HSPGs present on the cell surface (**Fig. 4**). Initial screening showed that CHO K1 cells expressed high levels of HS, whereas pgsD 677 cells were devoid of endogenous HS (**Fig. 4A**). In the absence of cell surface HSPGs, the amount of BMP-2 bound to the cell surface was greatly reduced (**Fig. 4A**). Notably, the addition of soluble GAG to CHO K1 cells reduces the amount of cell surface-bound BMP-2 (**Fig. 4B**). Heparin effectively prevents BMP-2 cell surface binding at 3 $\mu\text{g/mL}$ compared to the HSs, while HS5 is the least effective. However, pHS and bHS appear to be superior compared to heparin in modulating BMP-2 distribution at 30 $\mu\text{g/mL}$ dose. A similar trend was observed in C2C12 cells (data not shown).

Noggin activity is reduced in the presence of heparin or HS5

To determine the effect of GAG on noggin, which binds to and antagonizes BMP-2, we assayed ALP activity upon treatment of C2C12 cells with BMP-2, GAG and/or noggin. At 300 ng/mL, noggin inhibits BMP-2-induced ALP activity by 70% (**Fig. 5A**). In the presence of heparin or HS5, 300 ng/mL noggin only reduces BMP-2-stimulated ALP activity by approximately 20%. Meanwhile, pHS and bHS have negligible effects on noggin activity. Immunoprecipitation assays show that heparin and HS5 significantly reduce the interaction of noggin with BMP-2 (**Fig. 5B**).

HS5 does not promote BMP-2/BMPR-IA interactions

Apart from stabilizing BMP-2, GAGs may modulate BMP-2 interactions with its cognate BMPR-IA receptor. GAGs may promote receptor dimerization through its direct binding to BMP-2 as recently reported⁽³⁴⁾ and/or may modulate the binding of BMP-2 to its receptor, similar to what has been proposed for FGF2/FGFR interactions (34). Nitrocellulose dot blot assays with immobilized BMPR-IA and biotinylated GAG revealed that GAGs do not directly bind BMPR-IA (data not shown). Co-immunoprecipitation assays with BMPR-IA and BMP-2 indicate that, unlike HS5, heparin and other commercially available GAGs (i.e., pHS and bHS) slightly increase BMP-2/BMPR-IA interactions, although the experimental variation does not permit a definitive interpretation. This result further indicates biochemical differences between HS5 and the other GAGs tested, and that HS5 does not promote BMP-2 ligand-presentation to BMPR-IA (**Fig. 5C**).

HS5 has no anti-coagulant activity

As a fracture hematoma plays an important role in bone repair, we next determined the anti-coagulant activity of antithrombin (AT) in the presence of GAG (**Fig. 6**). Antithrombin pre-incubated with GAG was combined with Factor Xa (FXa). Any FXa that was not inhibited by the activated AT is able to cleave the chromogenic substrate S-2222 to release a chromophore. As expected, heparin (a known anti-coagulant) dose dependently activated AT resulting in the inhibition of FXa. In the presence of pHS or bHS, AT significantly reduced FXa activity, but only at 3 μ g/mL, whereas HS5 did not activate AT at any doses tested.

HS5 enhanced BMP-2-induced bone formation in a rat ectopic model

All rats survived the surgeries and healed uneventfully. The control resulted in negligible bone formation as ascertained by all the post-implantation analyses. Two-dimensional x-ray analyses revealed that all other treatments containing BMP-2 exhibited varying degrees of bone mineralization, indicated by the deposition of irregularly-shaped nodules (**Fig. 7A**). This was verified by 3D μ -CT examination. We picked a pre-determined threshold that resembles denser, cortical bone as this would be of direct clinical relevance. Notably, the combination of BMP-2 with HS5 resulted in 2-folds more bone volume than BMP-2 treatment alone and ~1.5 folds more bone than treatments containing heparin or bHS (**Fig. 7B**). The corresponding 3D images concur with the cortical bone values obtained.

H & E-stained sections of all BMP-2-treated groups revealed the presence of osteoblasts on the surface of woven bone trabeculae, and the deposition of mature bone (with osteocytes in lacuna) adjacent to bone marrow elements, with the ones containing HS5 treatment clearly exhibiting the most (**Fig. 7C**). Modified tetrachrome-stained sections confirmed the above H & E findings. The sections stained deep blue with bright red patches and this is indicative of an osteoid layer with lamellar bone. Markedly, HS5 treatment resulted in a higher incidence of lamellar bone. Collectively, our *in vivo* data suggests that HS5 therapy, in combination with BMP-2, stimulated robust bone mineralization in a rat ectopic model.

Discussion

The extreme charge density in heparin⁽³⁵⁾ tolerates interactions with a plethora of growth and adhesive factors as well as cationic elements^(16,22,36-38) that may run counter to the bone anabolic effect of BMP-2. Accordingly, we find that despite a favorable short-term effect, heparin does not potentiate BMP-2-dependent tissue mineralization *in vitro* or *in vivo*. Here we have characterized a heparan sulfate variant with sustained BMP-2-dependent osteogenic activity and minimal side effects.

Niche-specific HSs augment the generation and maintenance of hematopoietic stem cells⁽³⁹⁾ as well as enhance osteoblast development⁽⁴⁰⁾ and bone repair⁽⁴¹⁾. Our group has previously isolated a bone marrow-derived HS that supports hematopoietic cytokines in the *ex vivo* expansion of hematopoietic stem cells, by specifically increasing the number of myeloid lineage-committed progenitor cells⁽²⁴⁾. Hematopoietic stem cells are known to direct cell-fate decisions toward the osteogenic lineage through the secretion of BMP-2 and -6 into the bone marrow microenvironment⁽⁴²⁾. Thus, HS derived from the bone marrow microenvironment represents a physiologically relevant source that is likely to support factors involved in osteogenesis.

In the present study, we demonstrate that marrow-derived HS (HS5) is an effective adjuvant of BMP-2. HS5 can bind BMP-2 and augment BMP-2-induced bone formation to generate a mature lamellar structure containing dense mineralized regions akin to cortical bone. Furthermore, HS5 lacks the anticoagulant activity present in heparin. Heparin's anticoagulant activity has been attributed to its interaction with antithrombin through a unique 3-O-sulfated pentasaccharide motif⁽⁴³⁾. This 3-O-sulfate group is uncommon in HS⁽⁴⁴⁾. Consequently, only a small percentage of naturally occurring HS is able to bind to antithrombin and promote anticoagulation⁽⁴⁵⁾. Even though we were not able to confirm the absence of 3-O sulfation in HS5 due to the lack of appropriate disaccharide standards, data from the anticoagulation assay suggests minimal presence.

Mechanistically, HS5 sustains BMP-2 activity in a similar fashion to heparin by (i) prolonging its half-life, (ii) decreasing interactions with the BMP-2 antagonist noggin, and (iii) decreasing BMP-2 localization on cell surface HSPG. Cell surface HSPG is known to modulate the diffusion of BMP-2 and noggin into the extracellular space^(12,33,46). The interaction between HSPG and BMP-2 can lead to increased heteromeric BMP receptor assembly⁽³⁴⁾ and enhanced BMP signaling. It can also negatively regulate BMP-2 activity by facilitating BMP-2 internalization and reducing its availability to the receptor⁽³³⁾. Additionally, endogenous HSPG can confine noggin and its inhibitory effect in the pericellular environment⁽⁴⁶⁾. Thus the moderate disruption of BMP-2/HSPG interaction by HS5 as shown through our FACS data may positively regulate BMP-2 activity by decreasing BMP-2 internalization while minimizing disruption to BMP receptor assembly. Moreover, the decrease in the inhibitory effect of noggin by HS5 may not exclusively be through direct interference of BMP-2/noggin interaction as illustrated by our immunoprecipitation assay, but also by the delocalization of noggin and BMP-2 from the cell surface thereby diminishing its probability of complexing in the pericellular space.

In conclusion, the current work demonstrates the bioactivity and osteogenic ligand binding capacity of HS5. Co-administration of HS5 permits delivery of BMP-2 at lower and more physiological concentrations while retaining its osteogenic activity. The bone promoting biological function of HS5 may be linked to the unique degree and pattern of sulfation of GAGs from human bone marrow stromal cells. Compared to heparin that is derived from porcine intestinal mucosa, HS5 may be particularly adept at enhancing BMP-2 signaling while minimizing its effect on non-osteogenic factors. We are optimistic that further

characterization of GAGs may yield natural therapeutic compounds that greatly improve the efficacy of growth factors and osteogenic ligands used in bone regenerative medicine.

Acknowledgments

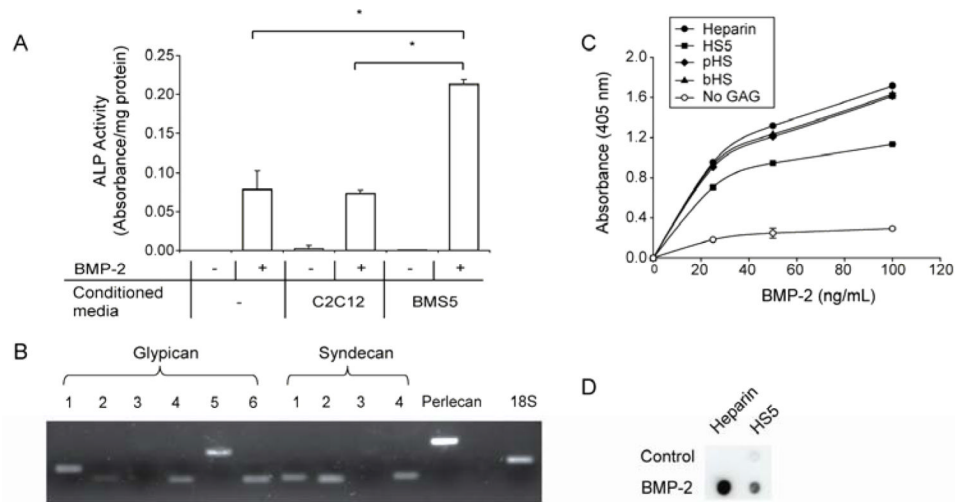
We acknowledge the grant support from Singapore's Agency for Science Technology and Research (A*STAR), the Biomedical Research Council of Singapore and the Institute of Medical Biology, Singapore.

References

1. Bishop GB, Einhorn TA. Current and future clinical applications of bone morphogenetic proteins in orthopaedic trauma surgery. *Int. Orthop.* 2007; 31(6):721–727. [PubMed: 17668207]
2. Dinopoulos H, Giannoudis PV. The use of bone morphogenetic proteins (BMPs) in long-bone non-unions. *Curr. Orthop.* 2007; 21(4):268–279.
3. Gautschi OP, Frey SP, Zellweger R. Bone morphogenetic proteins in clinical applications. *ANZ J. Surg.* 2007; 77(8):626–631. [PubMed: 17635273]
4. Garrison KR, Donell S, Ryder J, Shemilt I, Mugford M, Harvey I, Song F. Clinical effectiveness and cost-effectiveness of bone morphogenetic proteins in the non-healing of fractures and spinal fusion: a systematic review. *Health Technology Assessment.* 2007; 11(30)
5. Chung YI, Ahn KM, Jeon SH, Lee SY, Lee JH, Tae G. Enhanced bone regeneration with BMP-2 loaded functional nanoparticle-hydrogel complex. *J. Control. Release.* 2007; 121(1-2):91–99. [PubMed: 17604871]
6. Fu YC, Nie H, Ho ML, Wang CK, Wang CH. Optimized bone regeneration based on sustained release from three-dimensional fibrous PLGA/HAp composite scaffolds loaded with BMP-2. *Biotechnol. Bioeng.* 2008; 99(4):996–1006. [PubMed: 17879301]
7. Jeon O, Song SJ, Yang HS, Bhang SH, Kang SW, Sung MA, Lee JH, Kim BS. Long-term delivery enhances in vivo osteogenic efficacy of bone morphogenetic protein-2 compared to short-term delivery. *Biochem. Biophys. Res. Commun.* 2008; 369(2):774–780. [PubMed: 18313401]
8. Karageorgiou V, Tomkins M, Fajardo R, Meinel L, Snyder B, Wade K, Chen J, Vunjak-Novakovic G, Kaplan DL. Porous silk fibroin 3-D scaffolds for delivery of bone morphogenetic protein-2 in vitro and in vivo. *J. Biomed. Mater. Res. Part A.* 2006; 78A(2):324–334.
9. Takada T, Katagiri T, Ifuku M, Morimura N, Kobayashi M, Hasegawa K, Ogamo A, Kamijo R. Sulfated polysaccharides enhance the biological activities of bone morphogenetic proteins. *J. Biol. Chem.* 2003; 278(44):43229–43235. [PubMed: 12912996]
10. Esko, JD.; Linhardt, RJ. Proteins that bind sulfated glycosaminoglycans.. In: Varki, A.; Cummings, RD.; Esko, JD.; Freeze, HH.; Stanley, P.; Bertozzi, CR.; Hart, GW.; Ertler, ME., editors. *Essentials of Glycobiology.* Cold Spring Harbor Laboratory Press; La Jolla, California: 2008.
11. Zhao BH, Katagiri T, Toyoda H, Takada T, Yanai T, Fukuda T, Chung UI, Koike T, Takaoka K, Kamijo R. Heparin potentiates the in vivo ectopic bone formation induced by bone morphogenetic protein-2. *J. Biol. Chem.* 2006; 281(32):23246–23253. [PubMed: 16754660]
12. Paine-Saunders S, Viviano BL, Economides AN, Saunders S. Heparan sulfate proteoglycans retain Noggin at the cell surface - A potential mechanism for shaping bone morphogenetic protein gradients. *J. Biol. Chem.* 2002; 277(3):2089–2096. [PubMed: 11706034]
13. Arnander C, Westermark A, Veltheim R, Docherty-Skogh AC, Hilborn J, Engstrand T. Three-dimensional technology and bone morphogenetic protein in frontal bone reconstruction. *J. Craniofac. Surg.* 2006; 17(2):275–279. [PubMed: 16633175]
14. Gittens SA, Bagnall K, Matyas JR, Lobenberg R, Uludag H. Imparting bone mineral affinity to osteogenic proteins through heparin-bisphosphonate conjugates. *J. Control. Release.* 2004; 98(2): 255–268. [PubMed: 15262417]
15. Lin H, Zhaol Y, Sun WJ, Chen B, Zhang J, Zhao WX, Xiao ZF, Dai JW. The effect of crosslinking heparin to demineralized bone matrix on mechanical strength and specific binding to human bone morphogenetic protein-2. *Biomaterials.* 2008; 29(9):1189–1197. [PubMed: 18083224]

16. Atha DH, Stephens AW, Rosenberg RD. Evaluation of critical groups required for the binding of heparin to antithrombin. *Proc. Natl. Acad. Sci. U.S.A.* 1984; 81(4):1030–1034. [PubMed: 6583694]
17. Park SH, Silva M, Bahk WJ, McKellop H, Lieberman JR. Effect of repeated irrigation and debridement on fracture healing in an animal model. *J. Orthop. Res.* 2002; 20(6):1197–1204. [PubMed: 12472229]
18. Barbour LA, Kick SD, Steiner JF, LoVerde ME, Heddleston LN, Lear JL, Baron AE, Barton PL. A prospective study of heparin-induced osteoporosis in pregnancy using bone densitometry. *Am. J. Obstet. Gynecol.* 1994; 170(3):862–869. [PubMed: 8141217]
19. Muir JM, Andrew M, Hirsh J, Weitz JI, Young E, Deschamps P, Shaughnessy SG. Histomorphometric analysis of the effects of standard heparin on trabecular bone in vivo. *Blood.* 1996; 88(4):1314–1320. [PubMed: 8695849]
20. Chowdhury MH, Hamada C, Dempster DW. Effects of heparin on osteoclast activity. *J. Bone Miner. Res.* 1992; 7(7):771–777. [PubMed: 1642146]
21. Goldhaber P. Heparin enhancement of factors stimulating bone resorption in tissue culture. *Science.* 1965; 147:407–408. [PubMed: 14221490]
22. Irie A, Takami M, Kubo H, Sekino-Suzuki N, Kasahara K, Sanai Y. Heparin enhances osteoclastic bone resorption by inhibiting osteoprotegerin activity. *Bone.* 2007; 41(2):165–174. [PubMed: 17560185]
23. Esko JD, Selleck SB. Order out of chaos: Assembly of ligand binding sites in heparan sulfate. *Annu. Rev. Biochem.* 2002; 71:435–471. [PubMed: 12045103]
24. Bramono D, Rider D, Murali S, Nurcombe V, Cool S. The effect of human bone marrow stroma-derived heparan sulfate on the *ex vivo* expansion of human cord blood hematopoietic stem cells *Pharm. Res. Springer Netherlands.* 2010:1–10. December [Epub ahead of print].
25. Murali S, Manton KJ, Tjong V, Su XD, Haupt LM, Cool SM, Nurcombe V. Purification and characterization of heparan sulfate from human primary osteoblasts. *J. Cell. Biochem.* 2009; 108(5):1132–1142. [PubMed: 19777445]
26. Osmond RIW, Kett WC, Skett SE, Coombe DR. Protein-heparin interactions measured by BIAcore 2000 are affected by the method of heparin immobilization. *Anal. Biochem.* 2002; 310(2):199–207. [PubMed: 12423639]
27. Ng KW, Speicher T, Dombrowski C, Helledie T, Haupt LM, Nurcombe V, Cool SM. Osteogenic differentiation of murine embryonic stem cells is mediated by fibroblast growth factor receptors. *Stem Cells Dev.* 2007; 16(2):305–318. [PubMed: 17521241]
28. Rolny C, Spillmann D, Lindahl U, Claesson-Welsh L. Heparin amplifies platelet-derived growth factor (PDGF)-BB-induced PDGF alpha-receptor but not PDGF beta-receptor tyrosine phosphorylation in heparan sulfate-deficient cells - Effects on signal transduction and biological responses. *J. Biol. Chem.* 2002; 277(22):19315–19321. [PubMed: 11912193]
29. Yang HS, La WG, Bhang SH, Jeon JY, Lee JH, Kim BS. Heparin-conjugated fibrin as an injectable system for sustained delivery of bone morphogenetic protein-2. *Tissue Eng. Part A.* 2010; 16(4):1225–1233. [PubMed: 19886733]
30. Rai B, Lin JL, Lim ZXH, Guldborg RE, Hutmacher DW, Cool SM. Differences between in vitro viability and differentiation and in vivo bone-forming efficacy of human mesenchymal stem cells cultured on PCL-TCP scaffolds. *Biomaterials.* 2010; 31(31):7960–7970. [PubMed: 20688388]
31. Ralis ZA, Watkins G. Modified tetrachrome method for osteoid and defectively mineralized bone in paraffin sections. *Biotech. Histochem.* 1992; 67(6):339–345. [PubMed: 1283340]
32. Karamanos NK, Vanky P, Tzanakakis GN, Tsegenidis T, Hjerpe A. Ion-pair high-performance liquid chromatography for determining disaccharide composition in heparin and heparan sulphate. *J. Chromatogr. A.* 1997; 765(2):169–179. [PubMed: 9129307]
33. Jiao XY, Billings PC, O'Connell MP, Kaplan FS, Shore EM, Glaser DL. Heparan sulfate proteoglycans (HSPGs) modulate BMP2 osteogenic bioactivity in C2C12 cells. *J. Biol. Chem.* 2007; 282(2):1080–1086. [PubMed: 17020882]
34. Kuo WJ, Digman MA, Lander AD. Heparan sulfate acts as a bone morphogenetic protein coreceptor by facilitating ligand-induced receptor hetero-oligomerization. *Mol. Biol. Cell.* 2010; 21(22):4028–4041. [PubMed: 20861306]

35. Rabenstein DL. Heparin and heparan sulfate: structure and function. *Nat. Prod. Rep.* 2002; 19(3): 312–331. [PubMed: 12137280]
36. Goldsmith MW, Parry DJ. An investigation into the mechanism of the in vitro fall in rabbit plasma calcium which follows intravenous heparin injection. *Clin. Chim. Acta.* 1968; 19(3):429–38. [PubMed: 5643309]
37. Rabenstein DL, Robert JM, Peng J. Multinuclear magnetic resonance studies of the interaction of inorganic cations with heparin. *Carbohydr. Res.* 1995; 278(2):239–256. [PubMed: 8590444]
38. Shaughnessy SG, Young E, Deschamps P, Hirsh J. The effects of low molecular-weight and standard heparin on calcium loss from fetal-rat calvaria. *Blood.* 1995; 86(4):1368–1373. [PubMed: 7632944]
39. Gupta P, McCarthy JB, Verfaillie CM. Stromal fibroblast heparan sulfate is required for cytokine-mediated ex vivo maintenance of human long-term culture-initiating cells. *Blood.* 1996; 87(8): 3229–3236. [PubMed: 8605338]
40. Jackson RA, Murali S, Van Wijnen AJ, Stein GS, Nurcombe V, Cool SM. Heparan sulfate regulates the anabolic activity of MC3T3-E1 preosteoblast cells by induction of Runx2. *J. Cell. Physiol.* 2007; 210(1):38–50. [PubMed: 17051597]
41. Jackson RA, McDonald MM, Nurcombe V, Little DG, Cool SM. The use of heparan sulfate to augment fracture repair in a rat fracture model. *J. Orthop. Res.* 2006; 24(4):636–644. [PubMed: 16514633]
42. Jung YG, Song JH, Shiozawa Y, Wang JC, Wang Z, Williams B, Havens A, Schneider A, Ge CX, Franceschi RT, McCauley LK, Krebsbach PH, Taichman RS. Hematopoietic stem cells regulate mesenchymal stromal cell induction into osteoblasts thereby participating in the formation of the stem cell niche. *Stem Cells.* 2008; 26(8):2042–2051. [PubMed: 18499897]
43. Conrad, HE. Heparin-Binding Protein. Academic Press; San Diego: 1998.
44. Gorski B, Stringer SE. Tinkering with heparan sulfate sulfation to steer development. *Trends Cell Biol.* 2007; 17(4):173–177. [PubMed: 17320398]
45. Esko, JD.; Kimata, K.; Lindahl, U. Proteoglycans and sulfated glycosaminoglycans.. In: Varki, A.; Cummings, RD.; Esko, JD.; Freeze, HH.; Stanley, P.; Bertozzi, CR.; Hart, GW.; Etzler, ME., editors. *Essentials of Glycobiology.* 2nd ed.. Cold Spring Harbor Laboratory Press; La Jolla, California: 2008.
46. Viviano BL, Paine-Saunders S, Gasiunas N, Gallagher J, Saunders S. Domain-specific modification of heparan sulfate by Qsulf1 modulates the binding of the bone morphogenetic protein antagonist noggin. *J. Biol. Chem.* 2004; 279(7):5604–5611. [PubMed: 14645250]

**Figure 1.**

BMS5 conditioned media, which contains BMP-2-binding HSs, is able to enhance BMP-2-activity. (A) Conditioned media derived from BMS5 enhanced ALP activity induced by the addition of 100 ng/mL of BMP-2 for 3 days in C2C12 cells. (B) Various types of HSPG were expressed in BMS5 as revealed by its transcript expression profile. (C) BMP-2 bound to all GAGs tested in a dose-dependent manner using GAG binding plate, with HS5 showing the least capacity to bind BMP-2. (D) HS5 showed lower capacity to bind pre-adsorbed BMP-2 on a nitrocellulose membrane, which supported the GAG binding plate assay. Significant difference is represented as * $p < 0.05$.

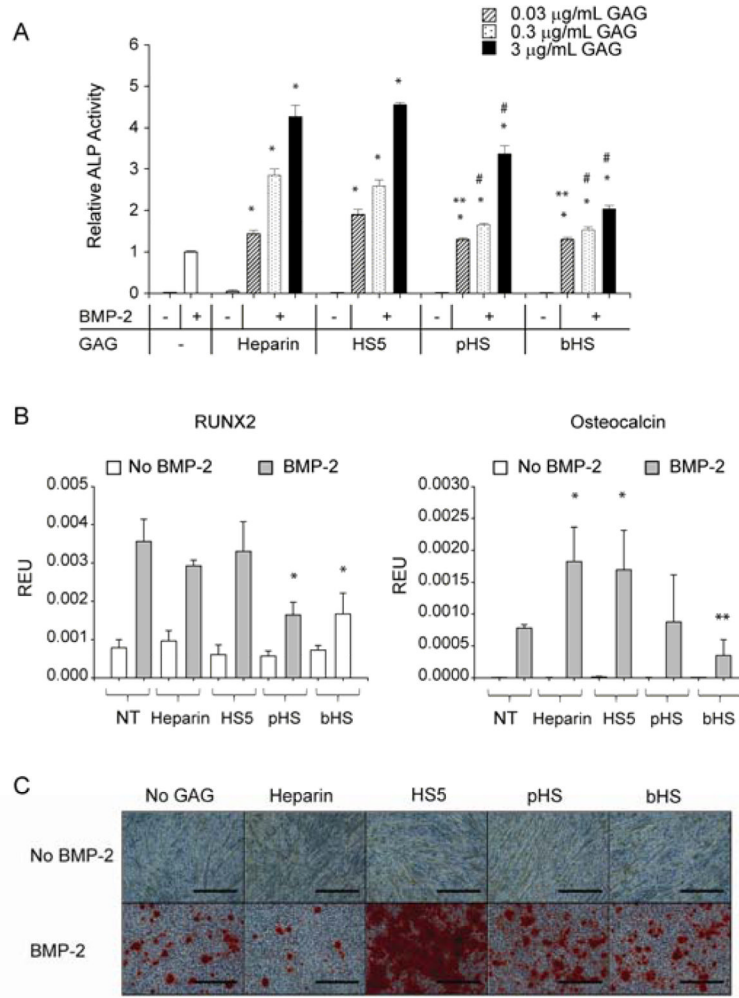


Figure 2. HS5 enhanced BMP-2-induced osteogenic differentiation in C2C12 cells. (A) All the GAGs dose-dependently enhanced BMP-2-induced ALP activity. HS5 showed comparable activity to heparin but was superior compared to pHS and bHS. (B) HS5 and heparin enhanced BMP-2-induced osteocalcin mRNA expression, presented here as relative expression unit (REU), but not RUNX2. C2C12 cells were cultured in the presence/absence of 100 ng/mL of BMP-2 with increasing amount of GAG (ALP assay) or 3 $\mu\text{g/mL}$ of GAG (transcript expression) for 3 days prior to harvesting the cells. (C) HS5 enhanced BMP-2 induced mineralization while heparin inhibited it. C2C12 cells were cultured in osteogenic media in the presence/absence of 100 ng/mL BMP-2 and 3 $\mu\text{g/mL}$ of GAG for 14 days prior to Alizarin Red staining, scale: 300 μm . Significant difference when compared to BMP-2 treatment alone is represented as * $p < 0.05$. Significant difference when compared to BMP-2 in combination with HS5 at equivalent dose is represented as ** $p < 0.05$, while with either heparin or HS5 at equivalent dose is represented as # $p < 0.05$.

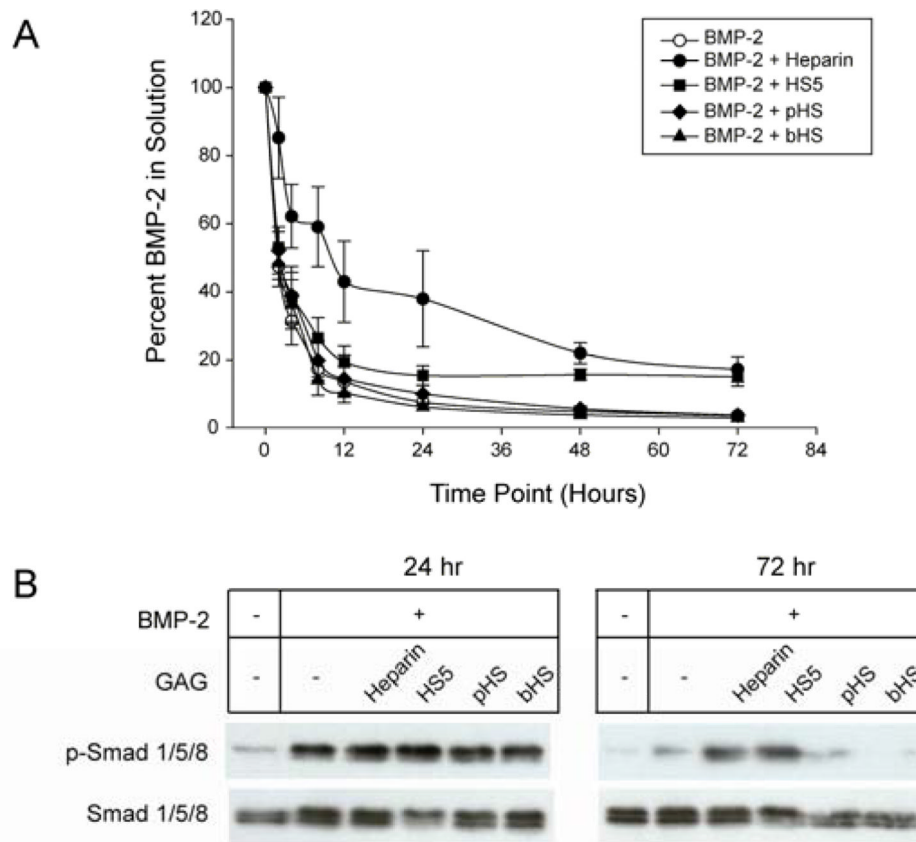


Figure 3. HS5 and heparin, but not commercial HSs, prolonged BMP-2 stability and activity. (A) BMP-2 stability over time was measured in a BMP-2 Quantikine ELISA kit. 100 ng/mL of BMP-2 was incubated in the presence/absence of 3 μ g/mL of GAG for up to 72 h. (B) BMP-2 incubated with heparin or HS5 for up to 72 h remained biologically active as indicated by its ability to induce Smad 1/5/8 phosphorylation (p-Smad 1/5/8) in C2C12 cells.

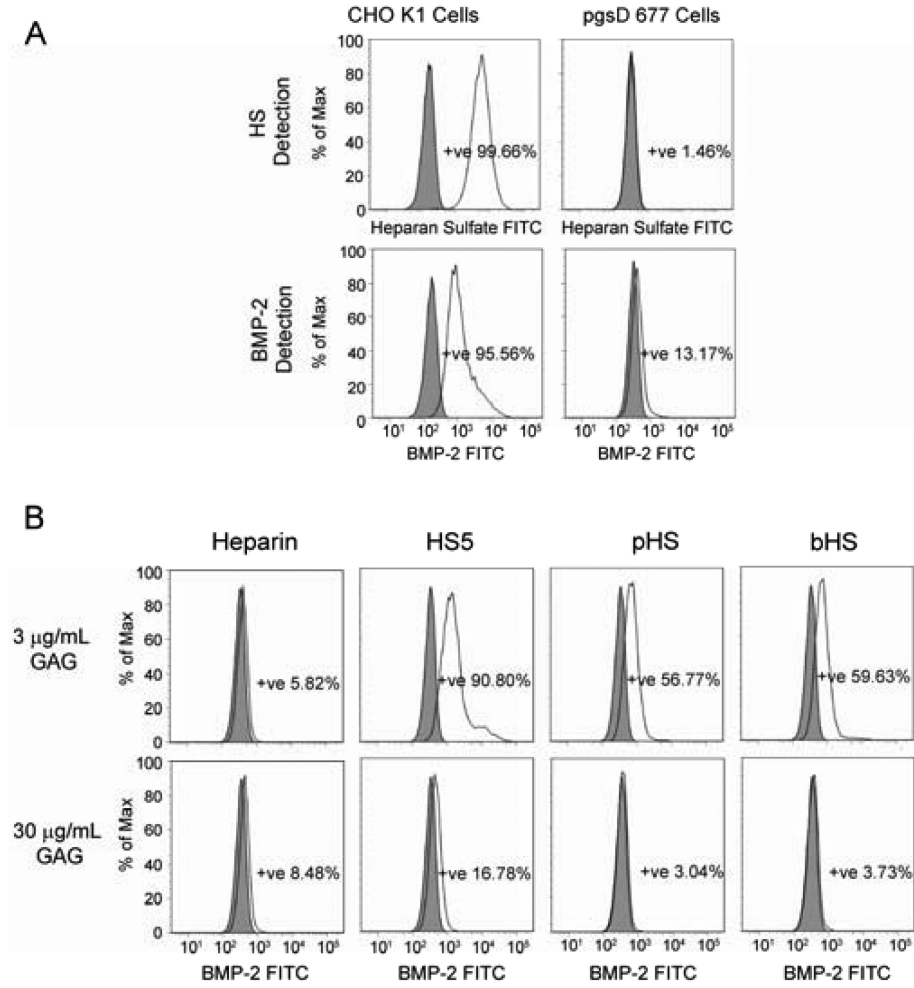


Figure 4. BMP-2 localization on the cell surface was modulated by endogenously expressed HSPGs and exogenously added GAG. (A) FACS analysis showed that endogenously expressed HSPGs play a significant role in localizing BMP-2 on the cell surface as confirmed in wild type (CHO K1) and HSPG-deficient (pgsD 677) CHO cells. (B) the addition of exogenous GAG reduced the amount of BMP-2 bound on the surface of CHO K1 cells dose dependently.

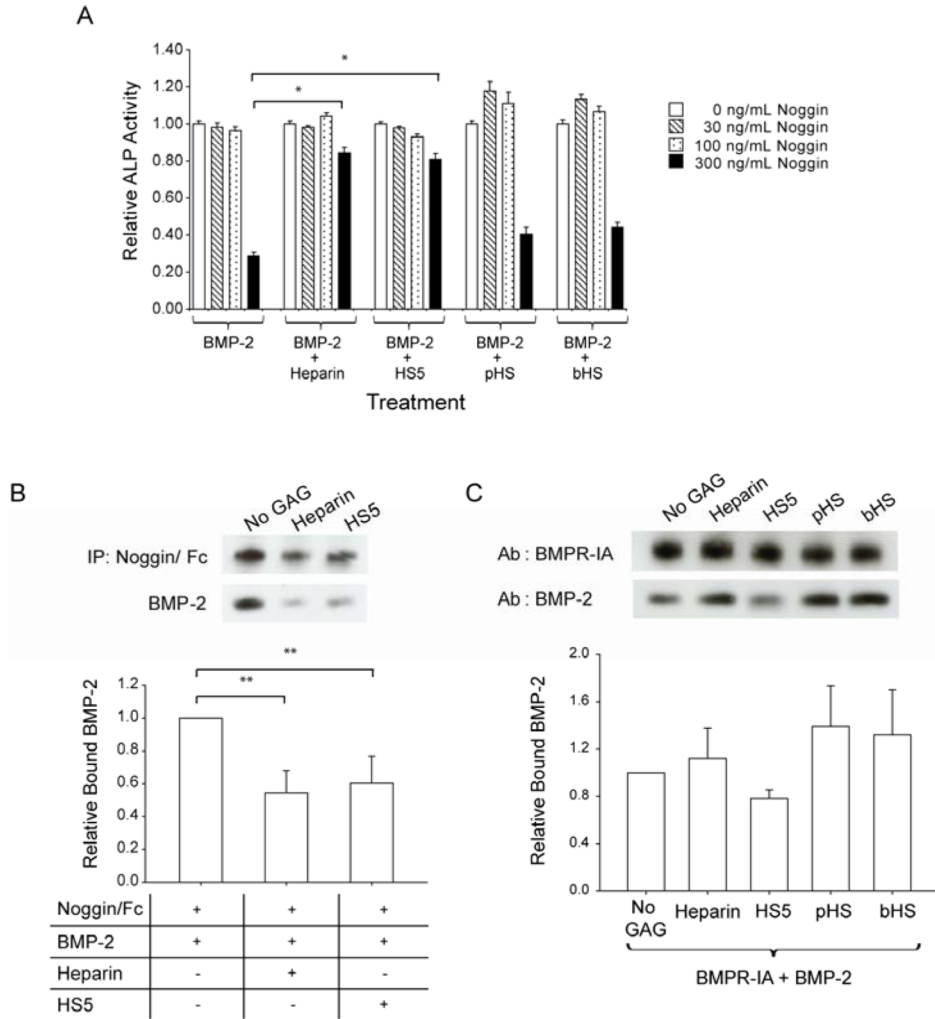


Figure 5. HS5 modulated BMP-2 interaction with noggin and reduced noggin's inhibitory effect toward BMP-2 activity, but had no effect on BMP-2/BMPR-IA interaction. (A) BMP-2 at 100 ng/mL was pre-incubated with or without 3 μ g/mL of GAG, and introduced to C2C12 cells for 3 days together with noggin at the indicated concentrations. Values were normalized to ALP activity observed in cells treated with BMP-2 in combination with each respective GAG in the absence of noggin. (B) 600 ng/mL of noggin/Fc was co-immunoprecipitated with 200 ng/mL of BMP-2 in the presence/absence of 6 μ g/mL of GAG. Densitometry analysis was derived from 3 separate blots. Relative bound BMP-2 was measured by normalizing the ratio derived from BMP-2 and noggin/Fc bands with that of the treatment group containing no GAG. (C) 100 ng/mL BMP-2 was co-immunoprecipitated with 640 ng/mL BMPR-IA/Fc in the presence/absence of 3 μ g/mL GAG and separated on a Western blot. Densitometry analysis was derived from 3 separate blots. Relative bound BMP-2 was measured by normalizing the ratio between the BMP-2 band and the BMPR-IA/Fc band with that of the treatment group containing no GAG. Significant difference is represented as * $p < 0.001$ and ** $p < 0.05$ when compared to treatment group containing no GAG.

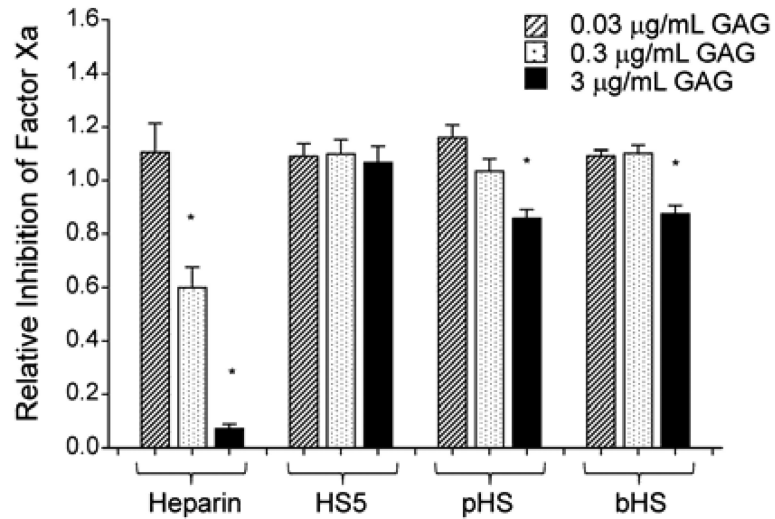
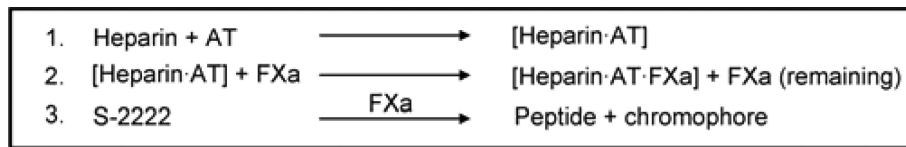


Figure 6.

HS has minimal anti-coagulant activity compared to heparin. At the indicated concentration, GAG was incubated with antithrombin (AT) before the addition of factor Xa (FXa). Any FXa that was not inhibited by AT was measured photometrically using chromogenic substrate S-2222. Relative inhibition was measured by normalizing the values to that of the treatment group containing no GAG. Significant difference is represented as * $p < 0.001$ when compared to the treatment group containing no GAG.

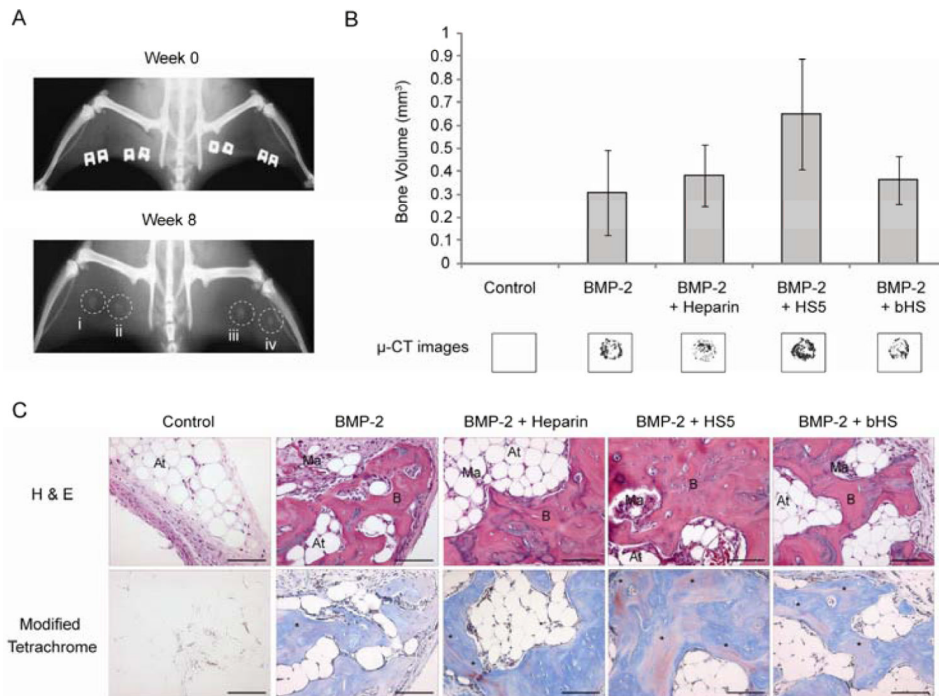


Figure 7. HS5 enhanced BMP-2-induced bone formation in a rat ectopic model at 8 weeks. (A) representative 2D x-rays of the rat hind limb muscle treated with BMP-2 alone (i) or in the presence of heparin (ii), HS5 (iii) or bHS (iv) revealed varying degrees of bone mineralization. (B) the bone volume (mm³), gated based on a pre-determined threshold that resembles dense cortical bone, and its corresponding 3D images showed that HS5 treatment resulted in higher levels of bone formation than the other groups, while no treatment (NT) showed absence of bone formation. This was determined by μ -CT analyses. Results are expressed as mean \pm standard deviation, n = 3 for each treatment. (C) Representative histological sections confirmed the abundance of lamellar bone in HS5 implants. Staining consisted of Hematoxylin/Eosin (H & E) and Modified Tetrachrome (blue = osteoid, red = bone). At: Adipose tissue, Ma: Bone marrow, B: Bone, *Lamellar bone, scale: 100 μ m.

Table 1

Disaccharide percentage composition of HS5 showed lower degree of sulfation compared to heparin. The area under each peak identified in the HPLC analysis was compared with the disaccharide standards to calculate the percentage composition of each disaccharides. Δ HexUA: uronic acid; GlcN: glucosamine; GlcNAc: N-acetyl-glucosamine; GlcNS: N-sulfated-glucosamine; 6S: 6O-sulfation; 2S: 2O-sulfation; n.d.: not detected.

No.	Disaccharide Standards	% Composition	
		HS5	Heparin ^a
1	Δ HexUA – GlcN	31.75	0.15
2	Δ HexUA-GlcNAc	n.d.	0.2
3	Δ HexUA – GlcN,6S	55.71	3.5
4	Δ HexUA,2S – GlcN	n.d.	n.d.
5	Δ HexUA – GlcNS	6.03	1.2
6	Δ HexUA – GlcNAc,6S	6.51	2.5
7	Δ HexUA,2S – GlcNAc	n.d.	1.5
8	Δ HexUA,2S – GlcN,6S	n.d.	2.35
9	Δ HexUA – GlcNS,6S	n.d.	12
10	Δ HexUA,2S – GlcNS	n.d.	4.7
11	Δ HexUA,2S – GlcNAc,6S	n.d.	3.9
12	Δ HexUA,2S – GlcNS,6S	n.d.	68.0

^aValues were adopted from Karamanos *et al.* (32).